University of Strathclyde Mechanical Engineering

THE UNIVERSITY OF STRATHCLYDE IN GLASGOW

DEPARTMENT OF MECHANICAL ENGINEERING

INVESTIGATION INTO THE EFFECT OF CAPSTAN SURFACE FINISH ON THE PERFORMANCE OF A SAILING WINCH

RUAIRIDH CAMERON-WHITE

MENG AERO-MECHANICAL ENGINEERING

2007

SUPERVISOR: DR ANDREW MCLAREN

TECHNICAL PAPER

3974 WORDS (EXCLUDING NOMENCLATURE, REFERENCES, FIGURES, GRAPHS, AND TABLES)

Abstract

The purpose of this project was to examine the effects of varying the surface finish of a sailing winch capstan on the friction between the drum and a standard sailing rope. As a result a sailing winch was designed and manufactured with the aim of having drums which could be interchanged simply.

The following four different winch drums were manufactured with varying surface patterns:

- Smooth Surface Finish
- Vertical Groove Finish
- Horizontal Groove Finish
- Knurled Surface Finish

Results for the produced sheet loads were found and the knurled and vertical groove patterns were shown to create the greatest sheet loads, whilst the horizontal groove and smooth surfaces proved to create similar forces. From the sheet loads the apparent coefficients of friction were established, and the results showed the knurled and vertical groove patterns had the higher coefficients of friction.

Lastly the repeatability of the experimental results was examined by looking at the mean standard deviations in the results. This established that large deviations in the results could be found when the winch required a greater force to be applied to the winch handle to make the rope slip, and put into question the repeatability of the results for these higher load occurrences.

Nomenclature

θ	Angle of wrap (Radians) (Contact angle of the rope around the capstan).
μ	Coefficient of friction.
σ	Mean Standard Deviation.
σ_{direct}	Direct stress acting on the sailing winch (N).
$\sigma_{bending}$	Bending stress acting on the sailing winch (N).
d_{drum}	Winch Drum Diameter (m).
F	Circumferential tension force (N).
FOS	Factor of Safety.
h	Height of winch drum (m).
I	2nd Moment of Area (m^4).
m	Moment (Nm).
N	Normal force of contact.
N_p	Number of Data Points.
R^2	Linear regression value.
T_s	Sheet Load (N).
T_t	Tailing Load (N).
$T_{.025}$	Statistical value for 95% confidence in the results.
W	Weight of winch operator (N).
$\bar{x}$	Mean data point value.
x_i	Data point value.
y	Position of neutral axis (m).

1. Introduction

Modern sailing yachts are very complex pieces of engineering, and can range from small and large cruising yachts to specialist racing yachts. They are all, however, designed to harness the power of the wind to propel the boat through the water by using sails and as a result yacht equipment has to be designed to withstand and control extremely large forces.

In order to control these forces one piece of yachting equipment of crucial importance is the sailing winch. The purpose of this project was to examine the effects of varying the surface finish of a sailing winch drum/capstan on the friction between the capstan and a standard sailing rope.

2. The Modern Sailing Winch

The modern sailing winch is used to mechanically reduce the force required by the sailor to control the sails. The capstan makes use of the static friction between the rope and capstans contacting surfaces to grip the rope and therefore allow the halyard or sheet, which control the sails, to be taken in.

The simplest, standard winch consists of a drum with a ratchet gearing system mounted on a set of bearings, and attached to the yacht. The rope (normally a sheet or halyard) is wrapped around the winch and a tailing load is provided on the free end of the rope by another crew member. The winch handle is inserted and used to rotate the drum to pull in the sheet.

There are a range of winches available on the market today, and these include, self tailing, and electrical or hydraulically powered winches. The variety of materials used in the manufacturing of winch drums is also quite extensive, and can be viewed below.

- Chromed Bronze
- Grey Anodised Alloy
- Bronze
- Stainless Steel
- Chrome

- Composite
- Carbon Fibre

There is very little information available on the surface finishes of these winch drum materials. However, work has been done on the effects of varying abraded finishes applied to a stainless steel surface on the friction and wear of carbon fibres in Roselman and Tabor [1]. The findings here suggested that friction was greater for the smooth surface finishes due to the carbon fibres used in this case conforming completely to the topography of the smooth finishes. For the abraded finishes this non conformation was therefore reducing the surface contact area between the fibre and surface.

3. Theory

3.1. Capstan Equation

The basic theory used by engineers to examine the friction between flexible fibre rope around a capstan and tensioned is the Capstan Friction Equation. Figure 1 below shows the Free Body Diagram for this system.

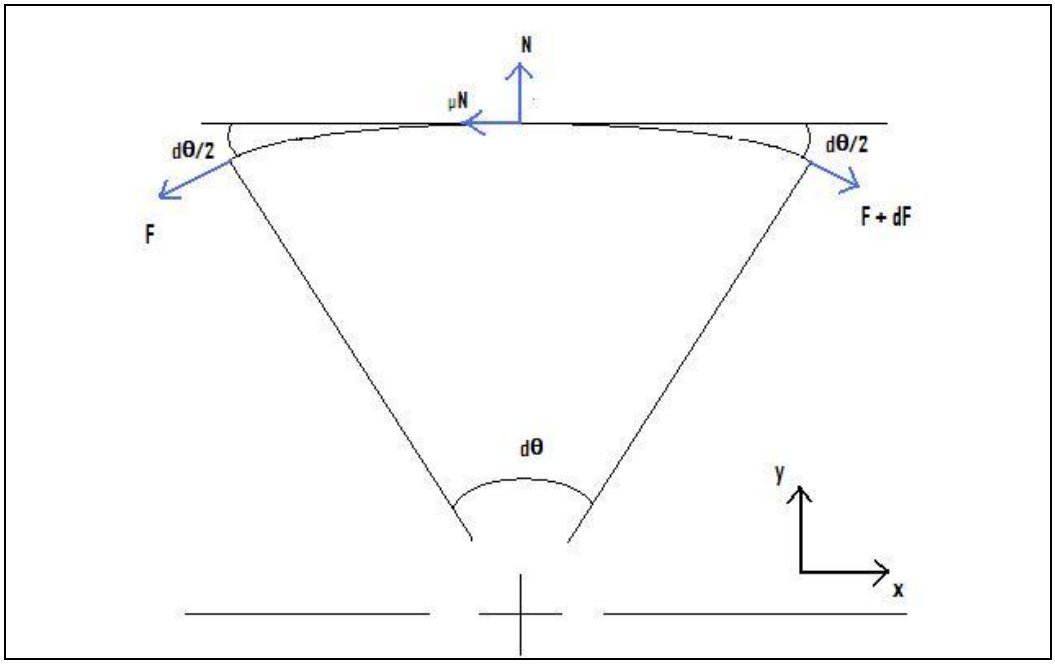

Figure 1: Capstan free body diagram.

The resultant capstan friction equation which was derived using Figure 1 is shown in Equation 1.

$$\boxed{T_s = T_t Exp(\mu\theta)}$$

Equation 1: Capstan Friction Equation

The Capstan Equation makes two distinct assumptions. Firstly, that friction is based on Coulomb Theory of Friction and this theory is designed for the study of two inflexible surfaces which is obviously not the case with a flexible fibre sailing rope. Secondly, the separate coils of the rope do not interact with one another when in a multi-turn configuration. There is unfortunately no published cohesive theory of friction which is applicable to this situation.

From reading published papers on related topics such as Budinski [2], and Albro and Liu [3], the applications which the capstan equation was applied to were only 180º or less in wrap angle. However the suitability of the capstan friction equation was confirmed in two previous years' projects, Fulton [4] and Campbell [5].

4. Test Rig

The basic equipment required for project was available from previous projects and was in reasonable working order. The basic components of the rig are shown in Figure 2 below, but with the new winch design attached.

Figure 2: Test rig with new designed winch attached.

The test rig consisted of the following components:

- Winch
- Sailing Rope
- Supporting Beam
- Load Cell

- Variable Angle Yoke
- Data Recording System
- Mass Hanger and Masses

In order to examine the suitability of the equipment for the project the following list of requirements was drawn up:

- Variable Angle Sheet Load
- Variable Tailing Load
- Data Recording System
- Accurate Force Measuring Device
- Changeable Winch Drum Surface

The above requirements were all met by the test rig from previous years' projects, apart from the Antal W8A size 8 alloy winch. Unfortunately this winch was not suitable for the project as it was decided after stripping down and examining the winch components that it was not possible to alter the winch drum surface in order to fulfil the testing requirements of the project. Therefore it would be necessary to design and build a winch from scratch.

4.1. Tailing Load Estimation

In order to find a value for the size of the tailing load to be provided by the mass hanger a simple experiment was carried out to find the force which a winch operator could apply to the tailing load end of the rope. This was done using a ZWICH 1445 material testing machine to which a rope was attached and to simulate the operation of a sailing winch the operator applied the same sort of force which would be applied as a tailing load. The pulling on the rope allowed the ZWICH 1445 to give a readout of the force being applied to the rope. This experiment was carried out firstly using one hand to simulate single person operation of a winch, and secondly two handed to simulate multiple person operation of a sailing winch. The experiment was repeated, for each simulation, fifteen times in order to compensate for fluctuations in the load being applied, and the mean of the force readings was used as the tailing loads which were rounded to the nearest 5lb. The results can be viewed in Table 1.

Testing Situation	Mean Resultant Force (N)	Mass (kg)	Mass (lb)	Tailing Load for Testing (lb)
1 Handed	70	7.1355759	15.73394	15
2 Handed	87	8.8685015	19.55505	20

Table 1: Tailing Load Testing Results

4.2. Load Cell Calibration

In order to check the working condition of the load cell before starting any experiments it was good practice to test the cell and therefore find its calibration.

The load cell was connected to a ZWICK rel 2061 tensile test rig. A testing program was then set to apply loads between 0kN and 3kN at intervals of 0.25kN which was the working range of the load cell. The cell was then plugged into its supply voltage and the Wheatstone bridge was connected to the data logging software. The workbench data logging software was set up to read the output voltage produced by the cell when loading was applied to it, and store these voltages and the time which they were produced. The testing was done 3 times, as standard practice dictated in calibration of equipment, in order to find an average for each of the voltages produced at the applied loads. The results from the calibration can be seen in Graph 1 below.

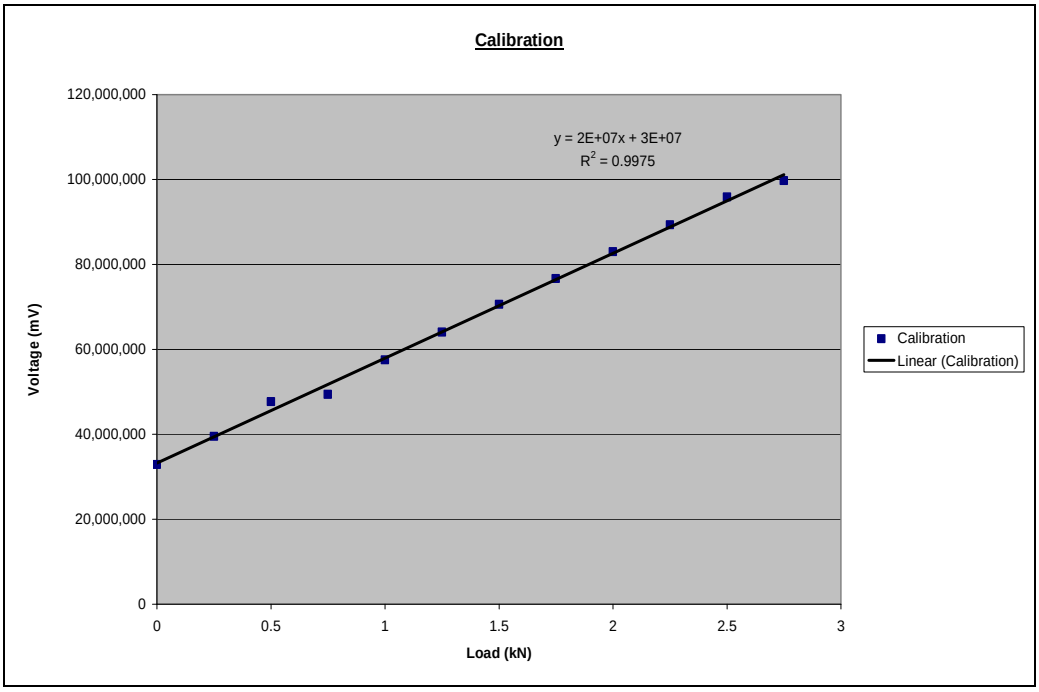

Graph 1: Load Cell Calibration

It can be seen in Graph 1 that the results are fairly linear, especially between 1kN and 2.75kN which shows the load cell to be working correctly within this range. However when examining loads less than 1kN on the graph it can be seen that they fluctuate slightly and after seeking consultation on this problem [6] it was discovered that it is not uncommon for strain gauges to experience problems at lower load ranges.

The formula for the linear trend line on the graph and its linear regression value were as follows:

$$\boxed{y = 2E + 07x + 3E + 07}$$

Equation 2: Equation of trend for Graph 1.

$$\boxed{R^2 = 0.9975}$$

Equation 3: Linear regression value.

$\therefore$

$$\boxed{Voltage = 2 \times 10^7 (Load) + 3 \times 10^7}$$

Equation 4: Relationship between load and voltage.

Equation 4 for the trend line describes the relationship between the load applied to the load cell and the resultant produced voltage. The linear regression value of 0.9975 which shows almost 100% of all the data points could be related to linear trend line, and that that load cell was operating correctly.

5. **Winch Design**

As stated in section 4 of the report, it was deemed necessary to design and manufacture a sailing winch from scratch for the project. The specifications for the winch design were as follows:

- Perform the basic features of a simple standard sailing winch.
- Have varying interchangeable winch drum surface finishes.

In order to simplify the winch design it was decided that the ratchet effect of the standard sailing winch was unnecessary in this application as the sheet load on the sailing winch would not have to be held. The priority of the design was to have interchangeable drum surface finishes and the following four finishes were decided on:

- Just machined finish.
- Horizontal grooved surface.
- Vertical grooved surface.
- Knurled surface finish.

Initial plans were drawn up and the designs were discussed and altered where necessary with consultation with the chief lab technician. The manufactured

winch is shown below in Figure 3, and the winch assembly drawing can be viewed in Appendix A.

Figure 3: Manufactured winch.

5.1. Stress Calculations

It was suggested by the lab technicians that the winch should be manufactured from aluminium in order to reduce the machining time, instead of the originally considered mild steel. In order to make sure that a winch manufactured from aluminium would be able to handle the forces being generated during the experimentation both the maximum stresses of the drum for direct and bending stress were calculated using Equations 5 and 6.

$$\sigma_{direct} = \frac{T_s}{\pi h d_{drum}}$$

Equation 5: Direct Stress

$$\sigma_{bending} = \frac{my}{I}$$

Equation 6: Bending Stress

The results from the calculations are shown in Table 2.

Maximum Sheet Load (kN)	3.602
Direct Stress (MPa)	0.104
Stress in Bending (MPa)	0.376
Aluminium Tensile Strength (MPa)	280 - 340
FOS for Direct Stress	2692.31
FOS for Stress in Bending	744.68

Table 2: Stress Calculation Results

It can be seen in the Table 2 that both the direct and bending stresses are greatly lower than the tensile strength for the En755-2 grade of aluminium [7] used in the manufacture of the winch, and that it gives rather large Factors of Safety (FOS) of 2692.31 and 744.68.

5.2 Winch Drum Design

There were four differing outer sleeve winch drums manufactured, all with varying surface finishes. The smooth drum was a just machined finish with no surface pattern added to it, and the knurled finish was produced in a lathe using a knurling tool. These differing drums can be viewed in Figure 4.

Figure 4: Vertical groove, knurled, smooth, and horizontal groove drum surface finishes.

During initial testing of the new winch it was discovered that the vertical groove and knurled surface patterns were cutting into the rope causing wear and damage and wear in fibres was shown to have a detrimental effect on the friction between surfaces and carbon fibres in Roselman and Tabor [1]. It was also making it impossible for the rope to slip for the angles of wrap of the rope around the drum greater and including 420º. The decision was then taken to dull the sharpness of the knurled and vertical surface patterns to try to reduce the grip on the rope which had varying success and shall be discussed later in the paper.

6. Testing

6.1. Testing Outline

As stated earlier in the thesis, the purpose of this project was to examine the effect of capstan surface finish on the performance of a sailing winch. This was done by testing each of the surfaces at various angles of wrap with a tailing load 15lb and then 20lb. Each test condition was repeated fifteen times to give an indication of the repeatability of the results and allow a better comparison between the results of the differing conditions.

In previous years' projects such as Campbell [5] and Walker [8] coil to coil contact was looked into and found to have a detrimental effect on the efficiency of a sailing winch, and rope to rope contact and the changing of cross sectional shape has been studied in papers such as Leech [9]. Therefore in order to simplify the rope and drum interaction every effort was made to ensure that the coils of the sailing rope would not come into contact with each other when in a multi-turn configuration.

6.2. Testing Procedures

The testing procedures were based and conformed to the American Society for Testing and Materials standards, ASTM G115-04 [10] and ASTM G143-03 [11]. The ASTM standards were used to ensure the experimental accuracy through correct procedures and practice. However the temperature and humidity experimental variables mentioned in these standards were deemed not to be of critical importance in the case of this project, as within the university laboratories these variables did not fluctuate enough.

Procedure:

1. Set up equipment.
2. Set destination file.
3. Start data recorder.
4. Wipe clean drum surface.
5. Set up number of wraps, making sure there is no rope to rope contact.
6. Suspend mass hanger and steady.
7. Turn winch handle till slippage of rope.
8. Unload the rope by removing tailing load.
9. Repeat steps 4 and 9 fifteen times.
10. Convert data and save in Excel worksheet.

6.3. Data Manipulation

Taking the results one tailing load at a time, the raw data from the experiments was initially converted from an ASCII file into an Excel spreadsheet. For each of the surfaces at the corresponding angles of wrap, the mean sheet load was found using the calibration equation. From this point the apparent coefficients of frictions were calculated using the capstan equation. The final part of the analysis required Equation 7 to be used to find the mean standard deviation for the data points.

$$t_{.025}\sigma = \sqrt{\frac{1}{N_p}\sum_{i=1}^{N_P}(x_i - \bar{x})^2}$$

Equation 7: Mean Standard Deviation

In order to give 95% confidence in the results for fifteen data points, using the table in Appendix B at a $t_{.025}$ value, the corresponding 2.131 was used in the calculation of the mean standard deviation.

From the resultant calculations, graphs were plotted displaying the angle of wrap, with the corresponding calculated sheet loads, and apparent coefficients of friction. On these graphs the mean standard deviations were displayed in the form of error bars to aid in the evaluation of the results.

7. Results

To begin with it should be noted that for that for the vertical groove surface, and knurled surface it was not possible to apply enough force to make the rope slip for angles of wrap of 780º and 810º. The results displayed in the graphs show the sheet load produced when the operator had applied their maximum force possible to the winch handle.

7.1. Sheet Load

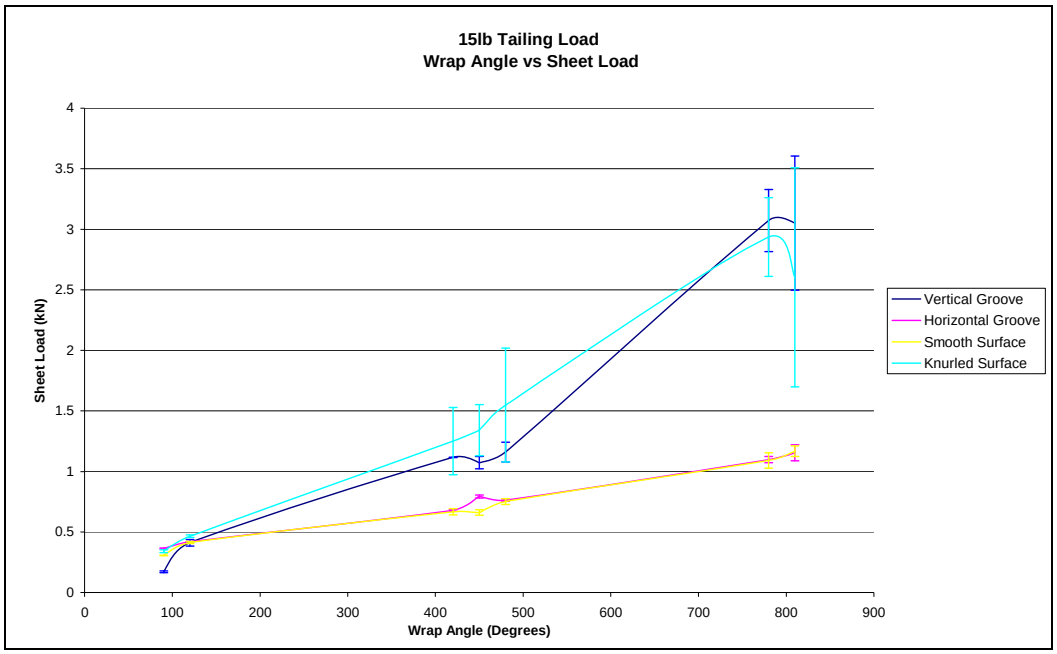

Graph 2: 15lb tailing load, wrap angle vs sheet load.

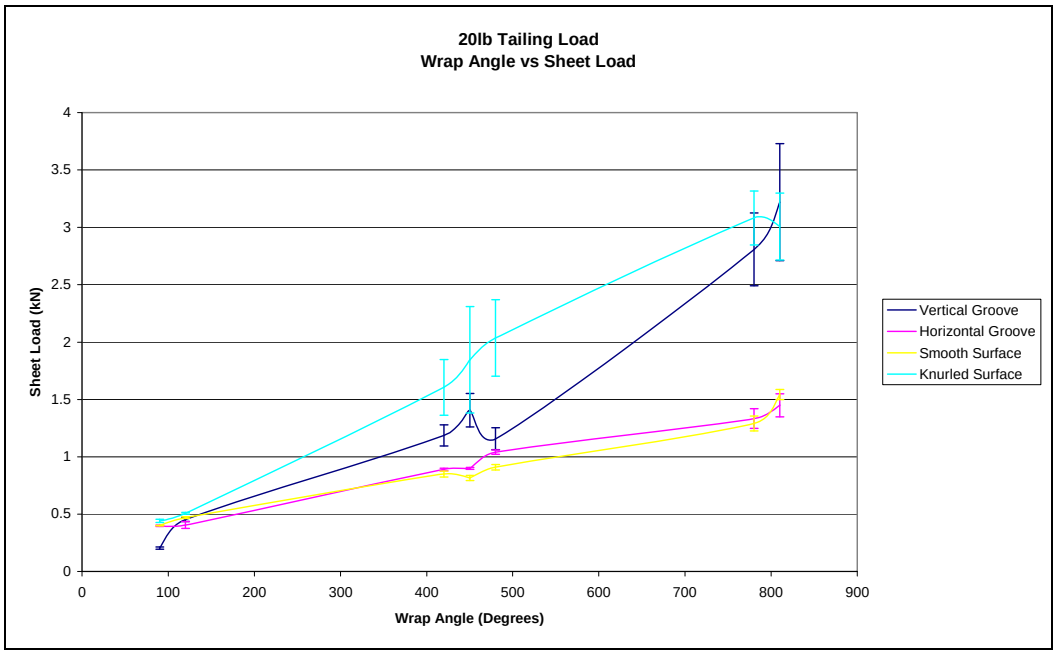

Graph 3: 20lb tailing load, wrap angle vs sheet load.

Graphs 2 and 3 display the resultant produced sheet load for each of the angles of wrap at the corresponding tailing load. In both of the charts the results of the calculation of 1 standard deviation in the experimental results are displayed in the form of error bars, and when taking into account the deviations graphs 2 and 3 both show the general trend of increasing sheet load for all surfaces as the angle of wrap is increased, which is as would have been expected, and that varying the winch drum surface finish does have an effect on the sheet load that the winch is able to produce. It can be seen on the graphs that for both tailing loads, in general, the knurled surface is able to allow the winch to produce that largest sheet loads. For each of the tailing loads the trends for the smooth and horizontal groove surfaces are fairly similar.

7.2. Apparent Coefficient of Friction

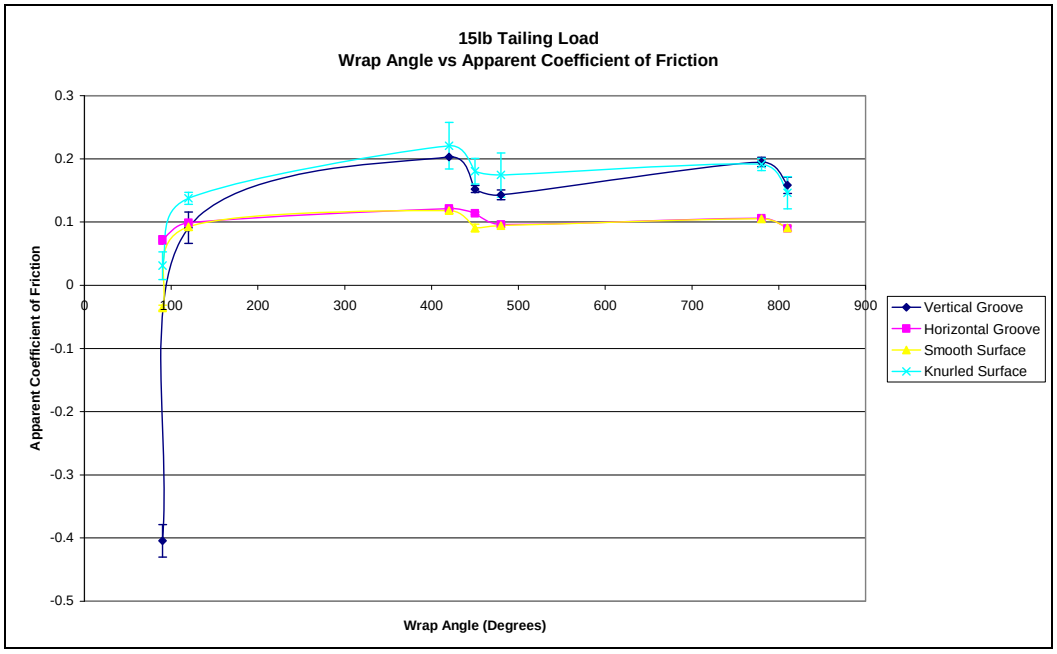

Graph 4: 15lb tailing load, wrap angle vs apparent coefficient of friction.

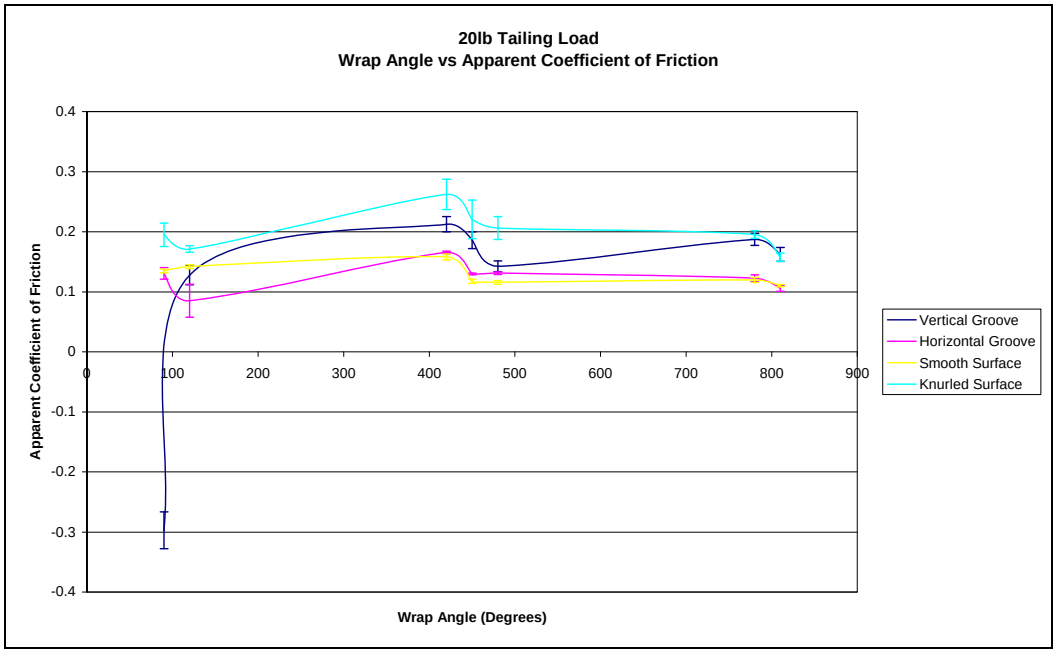

Graph 5: 15lb tailing load, wrap angle vs apparent coefficient of friction.

Graphs 4 and 5 both display the resultant produced apparent coefficient of friction for each of the angles of wrap at the corresponding tailing load. The knurled surface on both graphs is shown to have the greatest apparent coefficient of friction, and the trend lines for the smooth and horizontal pattered results are closely matched again. The trends on both graphs for all of the drums reach a maximum coefficient of friction at a 420º wrap angle, and then begin to decrease in value.

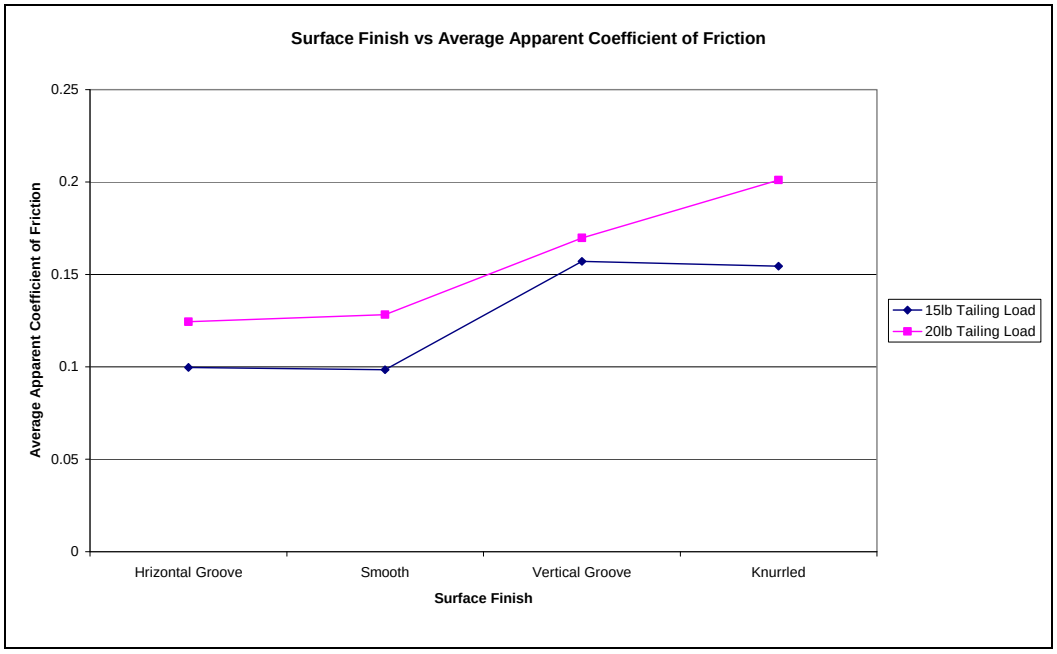

Graph 6: Apparent coefficient of friction summary.

The average values of the apparent coefficients of friction are displayed in Graph 6. It should be noted however, that the average results were calculated neglecting any negative values for the coefficients of friction. It can be seen on Graph 6 that increasing the tailing load results in an increase in the resultant coefficient of friction. For each of the tailing loads the results for the smooth and horizontal

groove surfaces are fairly similar, and the knurled and horizontal groove surfaces have greater coefficients of friction.

8. Discussion

As can be seen on Graphs 2, 3, 4, and 5, the standard deviation of the results are plotted in the form of error bars on the charts. Looking at all of the graphs in general the largest deviations in results are present in the vertical groove and knurled surfaces. This was due to the fact that these surfaces proved to have a greater hold on the rope as mentioned at the start of the analysis section of the report. This greater hold meant that the operator of the winch handle had to supply a large force when turning the winch handle in order to try to make the rope slip. Unfortunately trying to be consistent when applying these large forces proved to be quite difficult, and as a result the voltage outputs from the load cell were more scattered for these two drums compared to the smooth and horizontal groove surfaces. The deviations could also be attributed to wear of the rope on these surfaces, as the edges of the vertical groove and knurled surface tended to cut into the rope's surface damaging it. Whilst a great effort was taken to check for damage during the experimentation on a regular basis there would still be some damage to the rope which would go unnoticed which would have a detrimental effect on the efficiency of the interaction between the rope and drum surface.

There is the issue of the fluctuations in the produced sheet load and the apparent coefficients of friction results around the 450º angles of wrap and unfortunately the only explanation that can be given is that it could be due to flaws in the

experiment, or human error. What was expected to happen for the sheet load was that, as the angle of wrap was increased the load which could be produced by the winch on the sheet should have increased also, due to their being a greater area of the rope being in contact with the winch drum.

On Graphs 4 and 5 where there were negative coefficients of friction calculated from the Capstan Equation, the problem was due to the produced sheet load being less than the applied tailing load therefore giving a T_s/T_t value of less than one. When the natural log of this value was then found it produced a negative answer, resulting in the coefficient of friction being negative.

In Graph 6 the average apparent coefficients of friction are displayed for all of the various surfaces. When comparing the 20lb and 15lb tailing load results the 20lb load produced the more expected results for two reasons. Firstly, the 15lb tailing load knurled surface produced a smaller coefficient of friction than the vertical groove surface. This strange occurrence could be put down to the fact that during the experiment it was harder to make the rope slip for the higher angles of wrap for the rope and when the operator was applying the larger maximum force they could apply, it was very difficult to be consistent which is shown by the larger error bars in Graph 4. Secondly, the horizontal groove surface had a higher coefficient of friction than the smooth surface for a 15lb tailing load. It was expected that the horizontal groove would have the lowest coefficients of friction as the ropes surface tended to sit on the edges of the drums individual grooves, therefore having a smaller surface area of contact

between the winch drum and the rope. In Graph 6 for the 20lb tailing load this theory was confirmed, however when looking at the 15lb tailing load results this was shown not to be the case. The difference in the average coefficients of friction for these two drum surface for each of the tailing loads are very small for both tailing loads though.

As mentioned earlier the interaction between the vertical groove and knurled drum surfaces were causing damage to the rope. When looking at this issue from the perspective of a yachtsman this would be a major problem. On board a yacht, normally only a small same section of a rope would be in contact with a winch as it could be used to control, or pull in and out the sheet or halyard. This would mean that all of the rope wear would occur on the same small section of rope which could be 12m long, however this would be enough to render the whole rope incapable of performing its function. In the case of both the pleasure and racing yacht a winch causing a rope to wear out quickly would be not only be impractical and dangerous, but costly in the constant replacement of the rope. A balance in winch design must be found between the grip of the drums surface and the causing of wear on the rope, which was unfortunately was not achieved during this project.

9. Conclusion

The project was fairly successful in examining the effects of varying the surface finishes on the performance of a sailing winch. A working winch was designed and manufactured which allowed for the simple interchanging of outer winch drums meaning a variety of surfaces could be tested.

The results from the experiments show that the knurled and vertical groove surface patterns are able to produce higher sheet loads and apparent coefficients of friction as expected, including taking into account for the deviation in the results. The statistical analysis shown by the standard deviation calculations does however put the repeatability of the results in question, as for the higher rope angles of wrap there was difficulty in keeping the applied load to the winch handle constant due to the large forces required to be applied.

The other major factor affecting the results was the wear these more abrasive surface patterns were causing to the rope. Some of the wear, even though it was monitored, would go unnoticed which would have a bearing on the experimental results. This issue of wear also highlighted the practicality of some surface patterns for real life yachting applications where longevity of equipment is of importance.

References

[1] Roselman, I. C., and Tabor, D., The Friction and Wear of Individual Carbon Fibres, *Journal of Physics, Department: Applied Physics*, 1977, Vol. 10, 1181-1194.

[2] Budinski, K. G., Friction of Plastic Webs, *Tribology International*, 2001, 34, 625-633.

[3] Albro, C.S., and Liu, F., Effect of Groove Shape on the Frictional Hold of the Frictional Hold of a Sheave on Polyester Rope, *Transactions of the ASME: Journal of energy Resources Technology*, March 1985, Vol. 107, 103-106.

[4] Fulton, A., Investigation into the Effect of Rope to Rope Contact for a Winch in a Multi-Turn Configuration, University of Strathclyde, 2005.

[5] Campbell, P., Design and Construction of a Sailing Winch Simulator, University of Strathclyde, 2004.

[6] Consultation which Mr A. Crockett, Department of Mechanical Engineering, University of Strathclyde.

[7] CES, version 4.6.1, Materials Selection Program.

[8] Walker, M., Investigation into the effect of rope structure and materials on the performance of a standard sailing winch, University of Strathclyde, 2006.

[9] Leech, C. M., Modelling of Friction in Polymer Fibre Ropes, *International Journal of Mechanical Sciences*, March 2002, Vol. 44.

[10] ASTM Standards G115-04: 2006 Standard Guide for Measuring and Reporting Friction Coefficients.

[11] ASTM Standards G143-03: 2006 Standard Test Method for Measurement of Web/Roller Friction Characteristics.

Acknowledgements

I would like to express my many thanks and appreciation to the support and advice given to me by Dr A. J. McLaren throughout the project and for making himself available to answer any questions I had.

I would also like to take this opportunity to thank the university laboratory technicians for their help in the manufacturing, and testing of the experimental equipment. Special thanks are extended to Mr E. Duncan for his advice and help during the designing of the sailing winch, and Mr T. Farmer for manufacturing the winch itself.

Appendix A: Final Winch Design Drawings

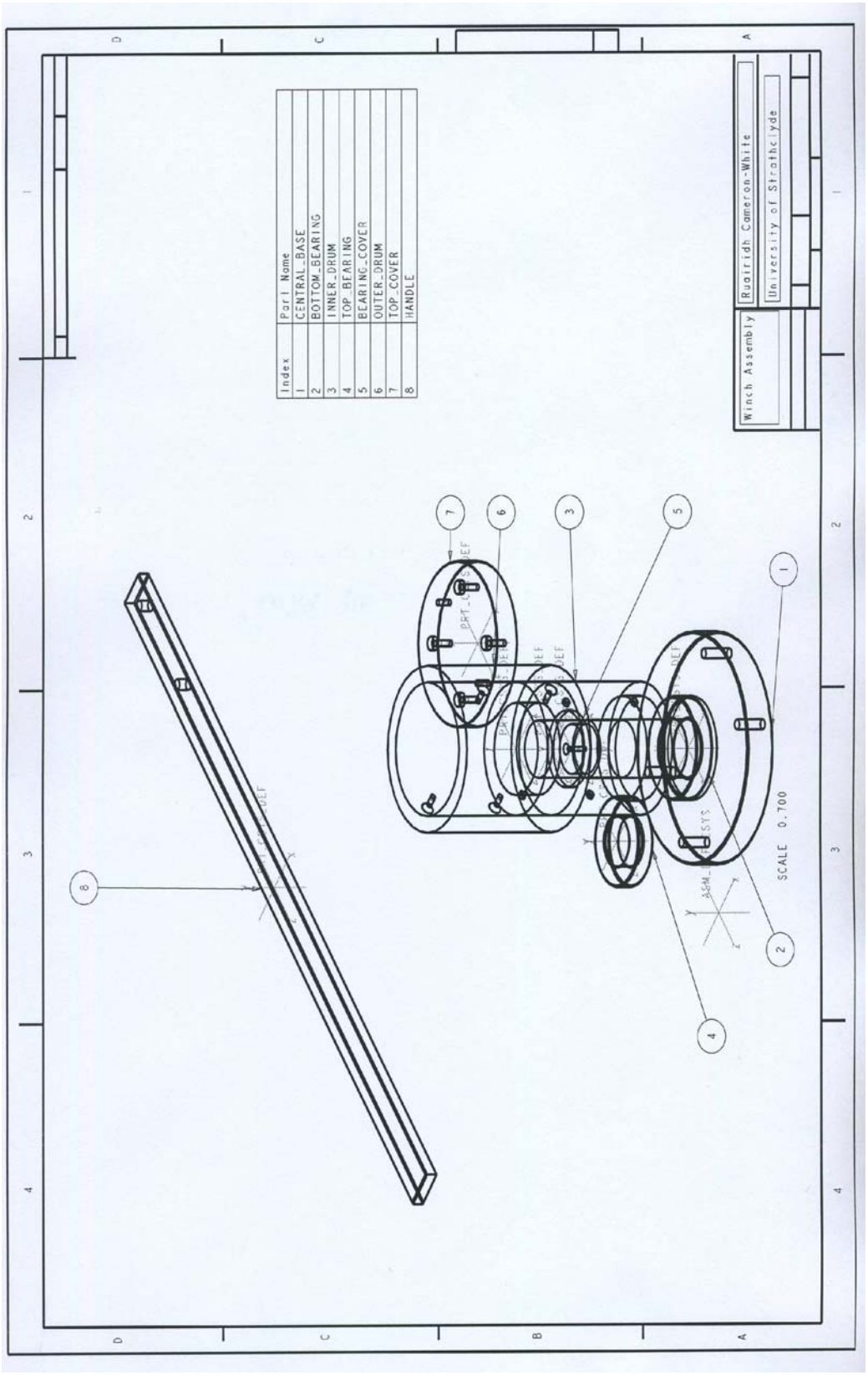

Appendix B: Experimental Statistical Data Table

Critical Values for Student's *T*

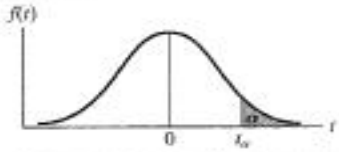

v	$t_{.100}$	$t_{.050}$	$t_{.025}$	$t_{.010}$	$t_{.005}$	$t_{.001}$	$t_{.0005}$
1	3.078	6.314	12.706	31.821	63.657	318.31	636.62
2	1.886	2.920	4.303	6.965	9.925	22.326	31.598
3	1.638	2.353	3.182	4.541	5.841	10.213	12.924
4	1.533	2.132	2.776	3.747	4.604	7.173	8.610
5	1.476	2.015	2.571	3.365	4.032	5.893	6.869
6	1.440	1.943	2.447	3.143	3.707	5.208	5.959
7	1.415	1.895	2.365	2.998	3.499	4.785	5.408
8	1.397	1.860	2.306	2.896	3.355	4.501	5.041
9	1.383	1.833	2.262	2.821	3.250	4.297	4.781
10	1.372	1.812	2.228	2.764	3.169	4.144	4.587
11	1.363	1.796	2.201	2.718	3.106	4.025	4.437
12	1.356	1.782	2.179	2.681	3.055	3.930	4.318
13	1.350	1.771	2.160	2.650	3.012	3.852	4.221
14	1.345	1.761	2.145	2.624	2.977	3.787	4.140
15	1.341	1.753	2.131	2.602	2.947	3.733	4.073
16	1.337	1.746	2.120	2.583	2.921	3.686	4.015
17	1.333	1.740	2.110	2.567	2.898	3.646	3.965
18	1.330	1.734	2.101	2.552	2.878	3.610	3.922
19	1.328	1.729	2.093	2.539	2.861	3.579	3.883
20	1.325	1.725	2.086	2.528	2.845	3.552	3.850
21	1.323	1.721	2.080	2.518	2.831	3.527	3.819
22	1.321	1.717	2.074	2.508	2.819	3.505	3.792
23	1.319	1.714	2.069	2.500	2.807	3.485	3.767
24	1.318	1.711	2.064	2.492	2.797	3.467	3.745
25	1.316	1.708	2.060	2.485	2.787	3.450	3.725
26	1.315	1.706	2.056	2.479	2.779	3.435	3.707
27	1.314	1.703	2.052	2.473	2.771	3.421	3.690
28	1.313	1.701	2.048	2.467	2.763	3.408	3.674
29	1.311	1.699	2.045	2.462	2.756	3.396	3.659
30	1.310	1.697	2.042	2.457	2.750	3.385	3.646
40	1.303	1.684	2.021	2.423	2.704	3.307	3.551
60	1.296	1.671	2.000	2.390	2.660	3.232	3.460
120	1.289	1.658	1.980	2.358	2.617	3.160	3.373
∞	1.282	1.645	1.960	2.326	2.576	3.090	3.291

Source: This table is reproduced with the kind permission of the Trustees of Biometrika from Pearson, E. S., and Hartley, H. O. (eds.) *The Biometrika Tables for Statisticians*, Vol. 1, 3rd ed., *Biometrika*, 1966.

Table used in Mean Standard Deviation Calculations
(Taken from Mendenhall, W., and Sincich, T., Statistics for Engineering and the Sciences, 5th Edition, New Jersey: Pearson Prentice Hall, 2007).